DLSU Research Congress 2024
De La Salle University, Manila, Philippines
June 20 to 22, 2024

Investigation on the Effect of Web Holes in the Compressive Strength of Cold-Formed Steel C-Sections

Bernardo Lejano[1*], Abigail Quiroga[2], Japheth Guico[2], Queenzie Ann Oropel[2]
[1] *Faculty Member, Department of Civil Engineering, De La Salle University*
[2] *BSCE Student, Department of Civil Engineering, De La Salle University*
**Corresponding Author: bernardo.lejano@dlsu.edu.ph*

Abstract: Cold-formed steel (CFS) is produced by cold-working processes, such as bending, pressing, or folding, carried out on cold thin steel plates or sheets. It is characterized by its high strength-to-weight ratio. These are often punched with holes to provide utility access for electrical and plumbing applications, but the reduced area affects its structural properties. Local provisions are mostly based on foreign codes, while research on locally manufactured CFS remain to be limited. Hence, this study investigated the effect of web holes on the compressive strength and buckling failure mode of locally produced CFS C-section members through experimental method and Code-based calculations. The compression test was performed using a hydraulic jack, load cell, and displacement transducers under pinned-pinned end conditions, while the computations were referenced from NSCP 2015 and AISI S100-16. A total of 39 specimens were tested, which cover two-hole sizes, two-hole counts, three-hole arrangements, and control. Experimental results found that hole lengths 8% to 16% of the member length produced a decrease in compressive strength. No definite effect was attributed to hole spacing or location, as hinted by the absence of these parameter in the Code, as the experimental strengths did not necessarily decrease as the holes near the member mid-height. Furthermore, all test specimens exhibited local and distortional buckling failures. The experimental strengths were comparable with the Code-predicted buckling strengths, which conservatively estimated strengths governing in local buckling. Hence, both the NSCP and AISI S100-16 are shown to provide safe design provisions for solid and perforated CFS members.

Key Words: cold-formed steel; compression test; buckling; C-section; axial strength

1. INTRODUCTION

Cold-formed steel (CFS) is one of the two structural steel types primarily used in construction due to its many advantages, such as its prominent high strength-to-weight ratio. In the local setting, the NSCP provides the regulations for the design of CFS based mainly on the AISI S100-07.

Although the design provisions for CFS update continually, several studies have shown some inconsistencies between the experimental and provision-based design values characterizing the structural performance of CFS (Li & Young, 2017; Chen et al., 2019; Xu, Shi, & Yang, 2014). In the Philippines, research is still lacking on its structural performance. Up to this point, this includes the axial strength investigation for solid C- and Z-sections, and

flexural strength for C-sections (Lejano, De Jesus, & Yu., 2020; Lejano & Ledesma, 2019). Current CFS standards in the country also lack provisions for sections with punched holes that are already present in the AISI S100-16. Furthermore, although the NSCP is deemed to be correct and safe when precisely followed, its development is based on foreign design codes which poses a potential difference in strength and performance of locally produced materials.

Hence, this study aimed to expand the local research on CFS by investigating the effect of varying web hole configurations in the compressive strength and failure modes of C-section members. The results obtained from experimental compressive tests and visual inspection were compared with the strength calculations of the NSCP and AISI S100-16.

2. METHODOLOGY

2.1 Research Design

This study analyzes the compressive strength and buckling failure modes of CFS C-section members. The experimental method involved concentric compressive load testing, while the computational method followed the strength calculations in NSCP and AISI. Visual inspections were also performed to verify the actual failure modes.

All members had a constant C-section of 89 x 32 x 10 x 0.8 mm and a length of 1000 mm. Solid members served as control specimens. The independent variables were the number, length, location, and spacing of the holes, while the dependent variables were the compressive buckling strength and failure mode. Shown in Table 1 is the list of the CFS specimens tested.

Table 1. Summary of hole parameters and specimens.

Label	Number	Location	Size	Replicate
HL0SP0	0	N/A	N/A	3
HL60SPT250	1	L/4	40x60	3
HL60SPT375	1	3L/8	40x60	3
HL60SPT500	1	L/2	40x60	3
HL80SPT250	1	L/4	40x60	3
HL80SPT375	1	3L/8	40x60	3
HL80SPT500	1	L/2	40x60	3
HL60SPC250	2	L/4	40x80	3
HL60SPC375	2	3L/8	40x80	3
HL60SPC500	2	L/2	40x80	3
HL80SPC250	2	L/4	40x80	3
HL80SPC375	2	3L/8	40x80	3
HL80SPC500	2	L/2	40x80	3
Total Number of Specimens				39

The labels in Table 1 were based on the hole length "HL" and hole arrangement "SPT" and "SPC", which also indicate the number of holes present, as a spacing from top (SPT) is applicable for members with a single hole while a spacing from the center (SPT) imply two holes. The shape of the holes and location of the holes are shown in Fig. 1. There were two-hole counts, three-hole locations, and two-hole sizes. Combining these cases, each with three replicates, sums up to 39 sample specimens (see Table 1).

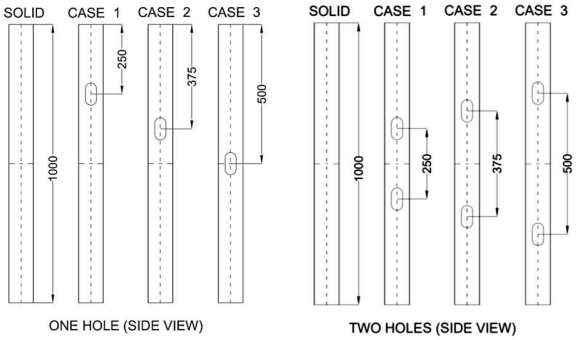

Fig 1. Location of Holes in CFS Specimens.

2.2 Materials and Equipment

The CFS C-section members were supplied and manufactured by a single local steel supplier. Though the steel sheets were imported from other countries or supplied by local major mills, the manufacturing process was done locally with the program of CNC machines based on the AISI standards, the same standard the NSCP was referenced from.

An experimental setup used to simulate concentric loading on the member was improvised using a hydraulic jack, metal end caps, and test frame. A load cell and two displacement transducers connected to a data logger were also used to monitor the axial resistance and displacement parameters used in analyzing the experimental strength.

2.3 Determination of Steel Properties

Prior to the experiment proper, six sample sheets were prepared and tested according to ASTM A370-20. The yield strength was obtained from tensile strength tests on the Universal Testing Machine. The resulting average strength of 338 MPa and elastic modulus of 203 GPa adopted from AISI S100-16 A3 were used in computing the code-based strengths.

2.4 Compressive Strength Test

The experimental setup in Fig. 2 followed the research conditions. The specimens were subjected to concentric loads in axial compression using a hydraulic jack until failure occurred.

Fig 2. Actual experimental setup.

Pin supports characterized the end connections for a simplified axial force calculation utilizing a ball and socket mechanism. The steel bearing ball also coincides with the centroid of the member to ensure concentric loading. A load cell was placed above the hydraulic jack for axial strength monitoring, while displacement transducers were attached to the center of the web approximately at mid-height and below the bottom end cap for lateral and axial displacement monitoring. During testing, high-speed cameras were used to observe and capture the buckling failure mode.

2.5 Computational Method

The computations followed the NSCP (National Structural Code of the Philippines) design specifications for CFS under Section 553 and Section C-1. Since the current NSCP only assumed solid members, the nominal strengths for perforated members were based on AISI (American Iron and Steel Institute) S100-16 Section E. While it was expected that local and distortional buckling modes would govern, as observed in the constant member length and past experiments, the yielding and flexural-torsional strength were still calculated for comparison. The lowest computed strength was concluded as the nominal axial strength of the member. To quantify the difference between computational and experimental results, the ratios between the two parameters were obtained.

2.6 Statistical Analysis

The significant difference between the compressive strength of solid and punched members were determined using the independent sample t-test in IBM SPSS Statistics software. Data visualization through scatter plots and regression analysis were also performed on the experimental and code-based strengths together with the hole parameters.

3. RESULTS AND DISCUSSION

3.1 Experimental Compressive Strength

The maximum compressive strength of each member was obtained from the data logger and averaged per case. This is summarized in Table 2. The solid members had an average strength of 17.205 kN. Out of all the one-holed members, the members with a 40x80 mm hole at L/2 had the lowest strength, but the members with a 40x60 mm hole at L/4 and 3L/8 had higher strengths than the solid member. This goes against the hypothesis that the strength decreases as the hole length increases. The unexpected strength increase may be due to the substantial difference between the hole length 60 mm and member length 1000 mm.

Table 2. Experimental compressive strengths.

Label	Count	Length	Location	P_{ave} [kN]
HL0SP0	0	N/A	N/A	17.205
HL60SPT250	1	60	L/4	17.372
HL60SPT375	1	60	3L/8	16.428
HL60SPT500	1	60	L/2	17.261
HL80SPT250	1	80	L/4	15.041
HL80SPT375	1	80	3L/8	15.651
HL80SPT500	1	80	L/2	14.597
HL60SPC250	2	120	L/4	14.985
HL60SPC375	2	120	3L/8	14.708
HL60SPC500	2	120	L/2	15.651
HL80SPC250	2	160	L/4	14.541
HL80SPC375	2	160	3L/8	14.430
HL80SPC500	2	160	L/2	15.596

It was also noted that the strength does not always decrease as the location of a single hole nears the mid-height. This was indicated by the horizontal trendline in Fig. 3. Similarly, the strength of two-holed members did not exhibit decrease as holes moved closer to the center for two-holed members.

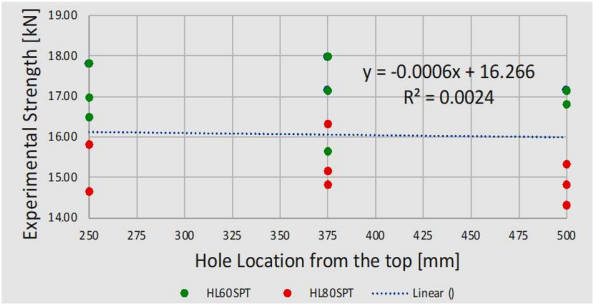

Fig 3. Experimental compressive strength of one-holed members vs hole location.

While hole location and spacing had no effect, the strength generally decreased from 17 to 14 kN as the hole number and hole length increases, as shown in Fig.4 and Fig.5. Members with hole lengths at least 8% of the member length had a strength reduction of at least 9%. Anything below had a strength close to the solid member, which was the case for members with only one 40 x 60 hole. The strength differences of these members were from 0.32% to -4.52%, unlike the rest of the cases that ranged from -9% to -16%.

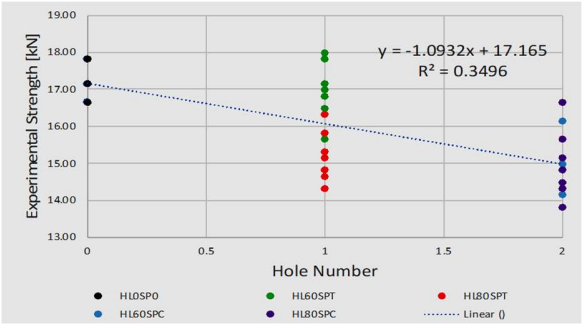

Fig 4. Experimental strength vs hole number.

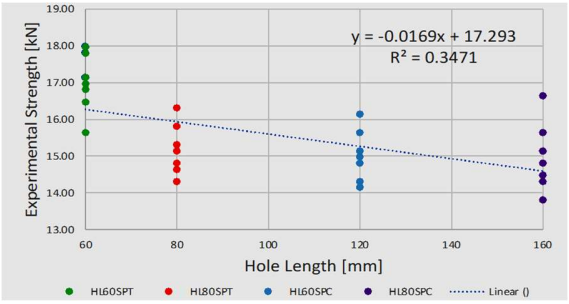

Fig 5. Experimental strength vs hole length.

To verify these results, the independent sample t-test was performed. It was concluded that one 40 x 60 hole regardless of the location has no significant effect on the compressive strength.

3.2 Code-based Compressive Strength

The 2015 NSCP, referenced from the AISI S100-07, determines the axial strength of concentrically loaded compression members as specified in Section 553. This main specification provides the nominal strength based on the governing resistance to two limit states: 1) Yielding, Flexural-Torsional or Torsional Buckling, and 2) Distortional Buckling. However, an alternative design method, the Direct Strength Method (DSM), provides calculations for another limit state of Local Buckling. The DSM also has similar general formulas for the first two limit states under Section 553.

Perforated CFS C-sections, however, are not considered in the current code despite their common and practical features. This limitation has been addressed in AISI S100-16 wherein the nominal axial strengths for punched members for the three limit states was provided. Table 3 shows the summary of the calculated nominal strengths for the three limit states based on the standard cross-sectional and material properties, namely the nominal flexural-torsional or torsional buckling strength P_{ne}, the nominal distortional buckling strength P_{nd}, and the nominal local buckling strength P_{nl}.

Table 3. Calculated nominal strengths.

Label	P_{ne} [kN]	P_{nd} [kN]	P_{nl} [kN]
HL0SP0	25.451	18.578	14.407
HL60SPT250	24.832	18.216	14.181
HL60SPT375	24.832	18.216	14.181
HL60SPT500	24.832	18.216	14.181
HL80SPT250	24.764	18.079	14.156
HL80SPT375	24.764	18.079	14.156
HL80SPT500	24.764	18.079	14.156
HL60SPC250	24.628	17.777	14.106
HL60SPC375	24.628	17.777	14.106
HL60SPC500	24.628	17.777	14.106
HL80SPC250	24.490	17.422	14.055
HL80SPC375	24.490	17.422	14.055
HL80SPC500	24.490	17.422	14.055

3.3 Experimental vs Code-based Compressive Strength

A comparison between the experimental and calculated nominal axial strengths based on the nominal sectional and steel properties is presented in Fig. 6. The experimental compressive strengths lie

above the governing strengths in local buckling, indicating that both the NSCP and the latest AISI S100 are conservative in predicting the compressive strength for the type of solid and perforated CFS members evaluated in this study.

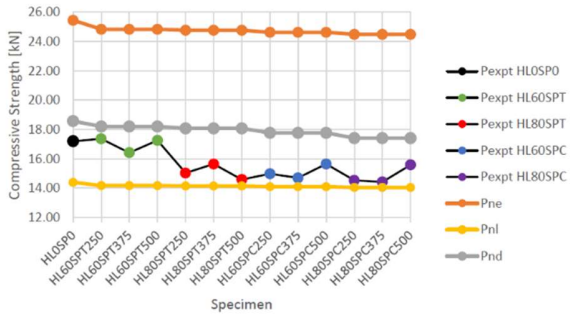

Fig. 6. Comparison between experimental and computational strengths.

In Fig. 7, P_{expt}, P_{nd}, and P_{nl} are compared. Plotted points above the equality line indicate conservative predictions as the experimental strengths exceed the predicted, while points below indicate nonconservative estimates. Meanwhile, the plot also shows a notable closeness of the predicted distortional buckling strengths to the equality line, which supports why the test samples also manifested distortional buckling.

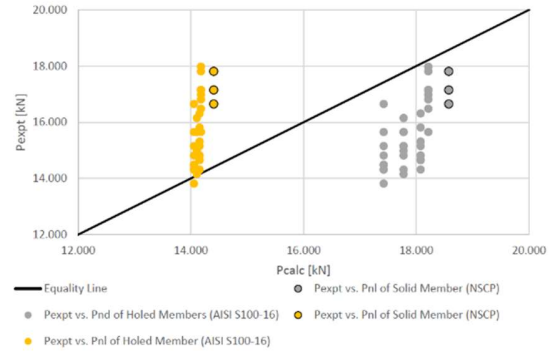

Fig. 7. Experimental vs. predicted Local Buckling P_{nl} and Distortional Buckling P_{nd} strengths.

3.4. Failure Modes

Through visual inspection of the tested samples, all specimens experienced local buckling and distortional buckling (Fig. 8 & Fig. 9). Since the sections had a constant length and thickness, the resulting modes of failure did not vary. For members with no holes, local buckling was identified approximately at the mid-height of the sample, as anticipated with a pinned-pinned boundary condition. On the other hand, for members with slotted holes, local buckling was most prominent around the location of the holes due to the reduced area and concentrated stress. Samples with two holes exhibited local buckling on only one hole while the other hole remained unbent.

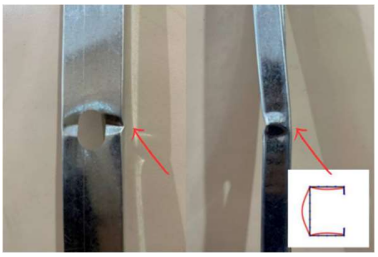

Fig. 8. Local buckling of samples with one hole.

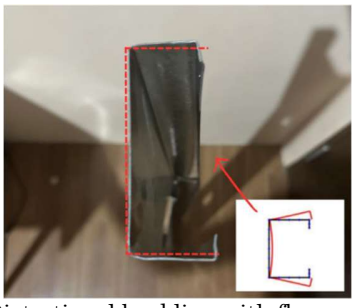

Fig. 9. Distortional buckling with flange rotation about the flange-web corners.

3.5. Load Displacement Curves

The lateral and axial displacements were obtained using displacement transducers and plotted against the compressive load. The general trend of the curves, as shown in Fig.10, the axial displacement was not affected by the hole parameters. All the load-axial displacement curves gradually increased from zero to the ultimate load before curving down, while the load-lateral displacement curve (Fig.11) immediately increases from zero to the ultimate load before sloping down gradually.

Increasing the hole number also increased the axial displacement but decreased the lateral displacement at ultimate load. Members with fewer holes or longer effective regions manage to reach higher axial displacements before failure, hinting an extended resistance than those with two holes or longer hole lengths.

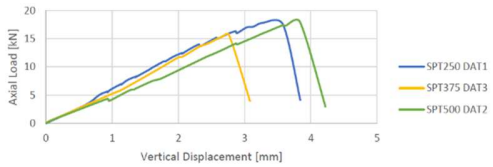

Fig. 10. Load-Displacement (Axial) Curves of HL60SPT.

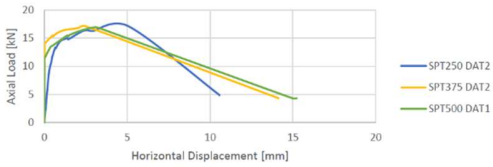

Fig. 11. Load-Displacement (Lateral) Curves of HL60SPT.

4. CONCLUSIONS

The study was able to make the following conclusions:

- There is a significant difference between the compressive strength of solid and punched members when the hole length is at least 8% of the member length. The strength generally decreased as the hole length and number increased from 60 to 160 mm and 0 to 2 holes.
- Hole lengths 8 to 16% of the member length reduced the compressive strength by 9 to 16%. The 16% strength reduction was found in members with the highest sum of hole lengths.
- Experimental results and supporting regression analysis showed that the hole location and spacing had no significant effect on the strengths, validating the absence of these parameters in strength computations.
- Both the NSCP and the latest AISI S100 are conservative in predicting the compressive strength for the type of solid and perforated CFS members evaluated in this study. All member specimens were predicted to fail in web local buckling.
- The failure modes were a combination of local and distortional buckling. Local buckling was observed to occur at the member mid-height for solid members and at the holed portion for punched members.
- Since the experimental compressive strengths neared the code-predicted distortional buckling strengths, it is concluded that distortional buckling took place shortly after local buckling.

5. ACKNOWLEDGMENTS

The authors would like to express their gratitude to the faculty and staff of the Civil Engineering Department of DLSU for their support, suggestions, and help, especially to the laboratory technician, Mr. Bernardo. Special appreciation is given to Mr. Jimmy Chan and his people at Accutech Steel and Maximetal Industries for supplying the materials needed for testing. The authors would also like to express their deepest gratitude to their friends and family for providing them with the resources and encouragement to carry out this research.

6. REFERENCES (use APA style for citations)

Chen, B., Roy, K., Uzzaman, A., Raftery, G. M., Nash, D., Clifton, G., Pouladi, P., & Lim, J. (2019). Effects of edge-stiffened web openings on the behaviour of cold-formed steel channel sections under compression. *Thin-Walled Structures, 144*, 106307.

Lejano, B., De Jesus, J., & Yu, A. (2020). Experimental compression tests of cold-formed steel (CFS) to verify its code-based strength. ASEAN Engineering Journal, 10(2). https://doi.org/10.11113/aej.v10.16600

Lejano, B., & Ledesma, E. (2019). Investigation of the flexural strength of cold-formed steel c-sections using computational and experimental method. GEOMATE Journal, 16(58), 55-61. https://doi.org/10.21660/2019.58.8139

Li, H. T., & Young, B. (2017). Tests of cold-formed high strength steel tubular sections undergoing web crippling. Engineering Structures, 141, 571–583.

Xu, L.., Shi, Y., & Yang, S. (2014). Compressive strength of cold-formed steel c-shape columns with slotted holes. International Specialty Conference on Cold-Formed Steel Structures, 4.https://scholarsmine.mst.edu/isccss/22iccfss/session02/4.